Heliyon 9 (2023) e23243

Contents lists available at ScienceDirect

Heliyon

journal homepage: www.cell.com/heliyon

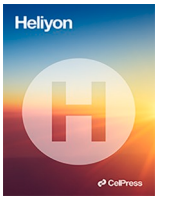

Exploring evolution characteristics of eco-environment quality in the Yangtze River Basin based on remote sensing ecological index

Zixi Liu [a], Weiwei Zhang [b,a,*], Huiyuan Lu [b], Jianwan Ji [b], Zhaohui Yang [b,a], Chao Chen [b]

[a] School of Environmental Science and Engineering, Suzhou University of Science and Technology, Suzhou, 215009, China
[b] School of Geography Science and Geomatics Engineering, Suzhou University of Science and Technology, Suzhou, 215009, China

ARTICLE INFO

Keywords:
Yangtze river basin
Google Earth Engine
Remote sensing ecological index
Geodetector
Eco-environment quality

ABSTRACT

As an important ecological-economic development area in China, scientific understanding of the spatial and temporal changes in eco-environment quality (EEQ) and its drivers in the Yangtze River Basin (YRB) is crucial for the effective implementation of ecological protection projects in the YRB. To address the lack of large-scale EEQ assessment in the YRB, this paper uses the Google Earth Engine (GEE) platform and the Remote Sensing Ecological Index (RSEI) to investigate the spatial and temporal characteristics of EEQ in the YRB from 2000 to 2020, and to analyze the impact of various factors on the EEQ of the YRB. This study showed that: (1) The overall EEQ of YRB was at the 'good' grade over the past 20 years, showing an increasing trend, with the value changing from 0.70 to 0.77. (2) The YRB's EEQ has positive spatial aggregation characteristics, with the northern part of the Jialing River basin and the Han River basin exhibiting a high-high aggregation type and the upper reaches exhibiting a low-low aggregation type. (3) In the past 20 years, the human activities had a greater impact on the EEQ of the YRB; moreover, all factors had a greater impact on the EEQ than a single factor. The interaction between the biological abundance index and population density had the most effect, with a q-value of 0.737 in 2020.

1. Introduction

Eco-environmental quality (EEQ) reflects the interaction degree between human activities and the natural environment [1]. It is a complex composition EEQ reflects the interaction degree between human activities and the natural environment [2]. It is a complex composite system including economy, society, and nature [3–5]. Based on the report issued by the United Nations in 2021, the global urban population is expected to reach 6.68 billion by 2050. However, accompanied by population accumulation, regional EEQ is facing higher pressure, which causes numerous ecological and environmental issues such as global warming [6–8], soil erosion [9], biodiversity loss [10], air pollution, and water pollution [11]. As a result, safeguarding regional EEQ is critical to improving human life quality and achieving regional sustainable development goals. In 2017, the Chinese government implemented the Regional Coordinated Development Strategy realize the purposes of regional sustainable development. Till now, China has paid increasingly more attention to dealing with eco-environmental issues by establishing EEQ standards, evaluating regional EEQ regularly, establishing nature reserves, and enacting legal documents. The level of regional EEQ could reflect the grade of regional ecological status. The

* Corresponding author. School of Geography Science and Geomatics Engineering, Suzhou University of Science and Technology, Suzhou, 215009, China.
E-mail address: zhangweiwei@usts.edu.cn (W. Zhang).

https://doi.org/10.1016/j.heliyon.2023.e23243
Received 22 September 2023; Received in revised form 29 November 2023; Accepted 29 November 2023
Available online 3 December 2023

assessment of the EEQ is the key step for creating countermeasures for the protection of the eco-environment and ensuring that relevant departments and the general public understand the significance of environmental protection, and the urgency and scale of environmental pollution problems [12]. The Yangtze River Basin (YRB) is an important watershed ecosystem in China, and monitoring the long-term trend of its EEQ and identifying areas where significant changes in EEQ have occurred, especially those where EEQ has deteriorated as well as those where it has improved, is an important task for the ecological protection of the YRB. At present, research on the assessment of the EEQ of the YRB mainly focuses on the middle and upper reaches or metropolitan areas, and a thorough and holistic assessment of the EEQ of the YRB is urgently needed.

Numerous studies have been conducted so far to analyze regional EEQ at various sizes using various variables. A single ecological indicator, such as vegetation coverage [13], a normalized difference vegetation index [14,15], a normalized building index [16], or land surface temperature, was frequently used to assess regional EEQ [17]. However, it is challenging to accurately describe the diverse EEQ's characteristics with one single indicator. In recent years, EEQ evaluation indicators have evolved from single indicators to composite indicators, considering the complexity of the eco-environment. To date, three models have been frequently applied to evaluate regional EEQ, namely: 1) the EEQ evaluating index; 2) the pressure-state-response model (PSR) [18,19]; and 3) the integrated assessment of ecological services and trade-offs [20,21]. The EEQ evaluating index can indicate the regional overall EEQ status but not reflect the regional EEQ status at any location. The two remaining models are difficult to compute and incapable of providing a quick assessment of the EEQ in a given region due to the difficulty of data acquisition. In response to these problems, Xu established a new remote sensing ecological index (RSEI) in 2013, which can be used to assess the regional EEQ by four main ecological aspects, namely greenness, wetness, heat, and dryness. Till now, this index has been used to assess the EEQ in different landscapes, such as urban [22], wetland [23], and basin [24]. To date, its effectiveness has been proven by numerous studies [25–28].

With the advantages of wide coverage, long-term monitoring, and multiple bands, remote sensing images have been a useful dataset for regional EEQ evaluation. Existing studies used Landsat images to construct the RSEI index and assess regional EEQ at various scales [29]. Landsat's surface coverage, however, is limited, making it challenging to evaluate large-scale EEQ. Compared with Landsat images, MODIS images could be used to evaluate the EEQ over a vast area due to their wide surface coverage. Rich remote sensing datasets have become easily accessible owing to Google's Google Earth Engine platform in recent years. The enormous cloud storage also reduces the time of downloading and processing data. This allows researchers to overcome the limitations of data acquisition, data storage, and low efficiency in processing traditional remote sensing analysis methods [30–32].

Currently, the water quality improvement of the Yangtze River is not reliable. The pollution in the coastal areas near the Yangtze River Delta (YRD) is still significant and extensive. The state of safeguarding and repairing the shorelines of the Yangtze River is still critical [33–35]. Most scholars, both at home and abroad, have analyzed and evaluated the EEQ of the YRB, but less attention has been paid to the driving factors affecting regional EEQ, and studies that use Point of Interest (POI) data as a driving factor to analyze EEQ are relatively rare [36] [–] [38]. At the same time, one of the study's breakthroughs is the combination of land cover status and RSEI analysis. In order to assess the distribution and trend of remote sensing ecological indexes in the YRB over the past 20 years, this study first utilized the GEE platform to preprocess the MODIS series image datasets from 2000 to 2020 for the YRB. The processing steps included the calculations of humidity, greenness, dryness, and heat index. Next, each index is rescaled to 0–1, and the RSEI is estimated using spatial principal component analysis (SPCA). Finally, potential indicators affecting the EEQ of the YRB were chosen, and the GeoDetector model is used to examine the key variables affecting regional EEQ. This study is structured as follows: Section materials and techniques describe the research topic, data source, and methodologies. Section results present the key findings from three perspectives: the section discussion presents the validation, implications, and limits; and the section conclusion presents the main findings of this study.

2. Materials and methods

In this study, a complete workflow diagram was created. First, we created five RSEI maps for 2000, 2005, 2010, 2015, and 2020 using the GEE platform MODIS data series. Second, the regional and temporal fluctuations, as well as the spatial correlations, of EEQ in the YRB were investigated. Finally, the RSEI was examined in conjunction with land cover status, and nine drivers influencing EEQ

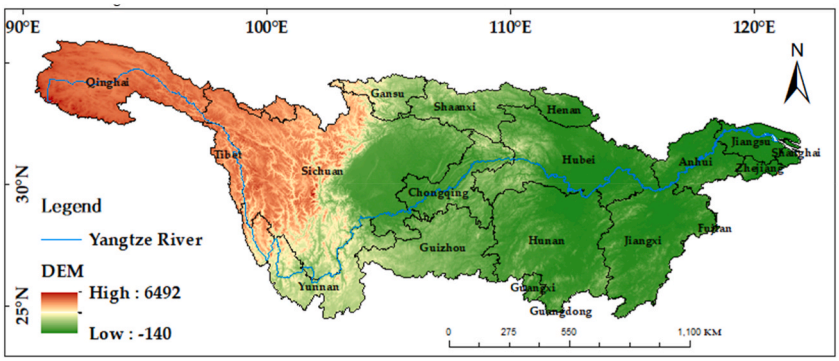

Fig. 1. The location map of the YRB.

were chosen, and the degree of effect of each driver on the watershed's EEQ was assessed using the GeoDetector.

2.1. Study area

The YRB, with a total area of 1.8 million square kilometers and accounting for 18.8 % of China's land area, is located between 90°33′-122°25′E longitude and 24°30′-35°45′N latitude (see Fig. 1). The Yangtze River has a mainstream of more than 6300 km and several tributaries; its lakes cover a total area of 15,200 square kilometers, accounting for about one-fifth of the country's total lake area. The average annual temperature of the YRB shows a distribution tendency of high in the east and low in the west, high in the south and low in the north. Most of the middle and lower reaches of the river have an average annual temperature of 16–18 °C, while the headwaters have an exceptionally low average annual temperature of −4 °C up and down. The YRB has an average annual rainfall of 1067 mm, while the annual rainfall in the headwaters of the river is less than 400 mm, which belongs to the desert zone, and most of the basin is between 800 and 1600 mm, which belongs to the humid zone.

The basin contains a quarter of the country's forests, and over 100 nature reserves have been established with a variety of conservation objectives. The area of lakes along the middle and lower reaches of the Yangtze River is 14,073 square kilometers, accounting for about 93 % of the total area of lakes in the YRB. Sichuan, Yunnan, Hubei and Jiangxi have the most forested areas, while nature reserves are mostly concentrated in the middle and lower reaches. The increase in glacial meltwater in the headwaters and upper reaches of the Yangtze River, influenced by climate warming, may lead to the shrinking or even extinction of lakes in the upper reaches of the Yangtze River, as well as the progressive degradation of the natural environment. Compared with the plateau glaciers in the upper reaches, the middle and lower reaches have more natural resources, more stable ecosystems and higher EEQ.

2.2. Data

The YRB's MODIS series of 2000, 2005, 2010, 2015, and 2020 from 1st May to 31st October, was the primary data source for this study. Because of the vast scope of this investigation and the huge unit of analysis, the MODIS series of remote sensing images was employed instead of Landsat imagery. These datasets included MOD11A2, and MOD09A1, which were used to derive essential characteristics including the normalized vegetation index, land surface temperature, and land surface reflectance. These datasets were obtained from the GEE cloud platform database. The Chinese Academy of Sciences' Resource and Environment Science and Data Center (https://www.resdc.cn/) offered elevation data, soil data, GDP and population spatial distribution, and data on land use remote sensing monitoring. The inverse distance weighting approach was employed to extrapolate the data. Meteorological data is based on the latitude and longitude of the weather stations, as well as the day-by-day data of the weather stations, which are interpolated by the inverse distance weighting method to obtain the day-by-day raster map of meteorological data on a nationwide scale, so as to compute the annual average temperature and precipitation data. The nighttime lighting data was acquired from Wu's findings [39].

2.3. Methods

2.3.1. Remote sensing ecological index (RSEI)

The creation of the remote sensing ecological index requires the use of four indicators: the greenness index (NDVI), humidity index (WET), dryness index (NDBSI), and heat index (LST) [40].

1. Greenness index (NDVI)

Using remote sensing data, calculate the difference between data from the near-infrared and red light bands. The Normalized Difference Vegetation Index (NDVI) is generally recognized as a good indicator of terrestrial vegetation productivity [41]. The calculation formula is shown in Equation (1):

$$NDVI = \frac{\rho_{\text{nir}} - \rho_{\text{red}}}{\rho_{\text{nir}} + \rho_{\text{red}}} \tag{1}$$

where ρ_{nir} and ρ_{red} indicate the reflectance of the NIR and red band respectively.

2. Humidity index (WET)

To reflect the moisture state of water bodies, topsoil, and vegetation, the moisture component calculated by the remote sensing tassel cap is utilized as a moisture indicator. The extraction of moisture components is possible using the following conversion coefficients for the MODIS data. The calculation formula is shown in Equation (2):

$$WET_{MODIS} = 0.2408\rho_{\text{blue}} + 0.3132\rho_{\text{green}} + 0.1147\rho_{\text{red}} + 0.2489\rho_{NIR} - 0.6416\rho_{SWIR1} - 0.5087\rho_{SWIR2} \tag{2}$$

where ρ_{green}, ρ_{blue}, ρ_{SWIR1}, and ρ_{SWIR2} indicate the reflectance of the green band, blue band, mid-infrared 1 band, and mid-infrared 2 bands.

3. Dryness index (NDBSI)

The Normalized Difference Built-up and Soil Index (NDBSI), which is calculated by averaging the Index-Based Built-up Index (IBI) and Soil Index (SI), is used to monitor dryness. The calculation formula is shown in Equations (3)–(5):

$$NDBSI = \frac{(SI + IBI)}{2} \tag{3}$$

$$SI = \frac{(\rho_{SWIR1} + \rho_{\text{red}}) - (\rho_{\text{blue}} - \rho_{NIR})}{(\rho_{SWIR1} + \rho_{\text{red}}) + (\rho_{\text{blue}} + \rho_{NIR})} \tag{4}$$

$$IBI = \frac{2\frac{\rho_{SWIR1}}{(\rho_{SWIR1}+\rho_{NIR})} - \left[\frac{\rho_{NIR}}{(\rho_{\text{red}}+\rho_{NIR})} + \frac{\rho_{\text{green}}}{(\rho_{SWIR1}+\rho_{\text{green}})}\right]}{2\frac{\rho_{SWIR1}}{(\rho_{SWIR1}+\rho_{NIR})} + \left[\frac{\rho_{NIR}}{(\rho_{\text{red}}+\rho_{NIR})} + \frac{\rho_{\text{green}}}{(\rho_{SWIR1}+\rho_{\text{green}})}\right]} \tag{5}$$

where ρ_{red}, ρ_{green}, ρ_{blue}, ρ_{nir}, and ρ_{SWIR1} indicate the reflectance in the red, green, blue, near-infrared, and mid-infrared1 bands.

4. Heat index (LST)

The heat index uses the LST_Day_1 km band of the MOD11A2 product. The MOD11A2 product provides an average 8-day land surface temperature (LST) in a 1200 × 1200-km grid. Each pixel value in MOD11A2 is a simple average of all the corresponding MOD11A1 LST pixels collected within that 8-day period. The 8-day compositing period was chosen because twice that period is the exact ground track repeat period of the Terra and Aqua platforms.

These four components are first normalized, and the normalization formula is presented in the equation, in accordance with the RSEI calculation method suggested by Xu [40]. The normalization formula is shown in Equation (6). Following normalization, these four components are then subjected to principal component transformation on the GEE platform. Principal component analysis may efficiently recombine variables such as greenness, humidity, heat, and dryness that have specific relationships into multiple components in order to accomplish data dimensionality reduction and noise isolation. The maximum information of each variable is included in the first principal component (PC1), and the information of the first principal component is retrieved as the information source of RSEI, which is expressed by $RSEI_0$, and ultimately, the normalization of $RSEI_0$ is RSEI.

$$N_i = \frac{I_i - I_{\min}}{I_{\max} - I_{\min}} \tag{6}$$

where N_i is the value of each indicator after normalization; I_i is the value of the indicator before normalization; $I_{\min}$ and $I_{\max}$ are the minimum and maximum values of the indicator before normalization, respectively.

2.3.2. Spatial autocorrelation analysis

Spatial autocorrelation, which consists of the two components global spatial autocorrelation and local spatial autocorrelation, quantifies the degree of connection between behavior in one area and the same phenomena in surrounding regional units. The global Moran's index (*Global Moran's I*) can demonstrate how the EEQ is geographically organized overall. The Moran's I values ranged from −1 and 1. When the values range from 0 to 1, there is a positive relationship between the geographical components. The closer the value is to 1 and -1, the higher the positive and negative correlation, respectively [42]. The following formula is the expression for *Global Moran's I:*

$$Global\ Moran's\ I = \frac{n\sum_{i=1}^{n}\sum_{j=1}^{n} W_{ij}(x_i - \overline{x})(x_j - \overline{x})}{\left(\sum_{i=1}^{n}\sum_{j=1}^{n} W_{ij}\right)\sum_{i=1}^{n}(x_i - \overline{x})^2} \tag{7}$$

Local spatial autocorrelation analysis was performed using *Local Moran's I* LISA to further reveal the aggregation of EEQ in the research region and understand the EEQ's local geographical distribution features. The following formula is the expression for *Local Moran's I*:

$$Local\ Moran's\ I = \frac{n(x_i - \overline{x})\sum_{j=1}^{n} W_{ij}(x_j - \overline{x})}{\sum_{i=1}^{n}(x_i - \overline{x})^2} \tag{8}$$

2.3.3. Biological abundance index (BAI)

Because land cover data is qualitative, while all other data is quantifiable, the BAI was employed as a driver rather than land cover data. The BAI is calculated depending on the area of each land cover type. The following formula is the expression for BAI:

$$BAI = A_{bio} \times \frac{0.35 \times x_1 + 0.21 \times x_2 + 0.28 \times x_3 + 0.11 \times x_4 + 0.04 \times x_5 + 0.01 \times x_6}{x_7} \quad (9)$$

which x1-x7 denote forest land, grassland, water, cropland, built-up land, unused land and total area of the region, respectively, and A_{bio} is the normalized index of biological abundance.

2.3.4. Geodetector

A technology called Geodetector is used to investigate spatially divergent geographic events. It has four detectors: ecological, interaction, factor, and risk detection [43]. Geodetector models could both identify spatial anisotropy and its causes. This approach has a beautiful form, no linearity presumptions, and a specific physical meaning, more importantly, it could detect the interaction degree of two or more factors, which had also been widely used [44–46]. Temperature, precipitation, elevation, population, GDP, type of soil, type of land use, and nighttime light data were chosen as independent variables in this study to quantify their influence on regional RSEI.

The q-value measures the association between the quality of the ecological environment (Y) and the risk and factor detection assessment index (X). The calculation formula is shown in Equation (10):

$$q = 1 - \frac{\sum_{h=1}^{L} N_h \sigma_h^2}{N\sigma^2} = 1 - \frac{SSW}{SST} \quad (10)$$

where h = 1, 2 …, L is the stratification of variable Y or factor X; N and N_h are the number of cells in the whole region and stratum h; σ_h^2 and σ^2 are the variance of Y values in stratum h and the whole region; SSW and SST are the sum of variance within the stratum and the total variance in the whole region. The more significant the value, the greater the influence of evaluation index X on evaluation index Y.

There are times when the effects of the independent variables on the dependent variable are independent of one another, and interaction detects the interaction between various factors and assesses whether the interaction effect between the two independent variables increases or decreases the explanatory power of the dependent variable.

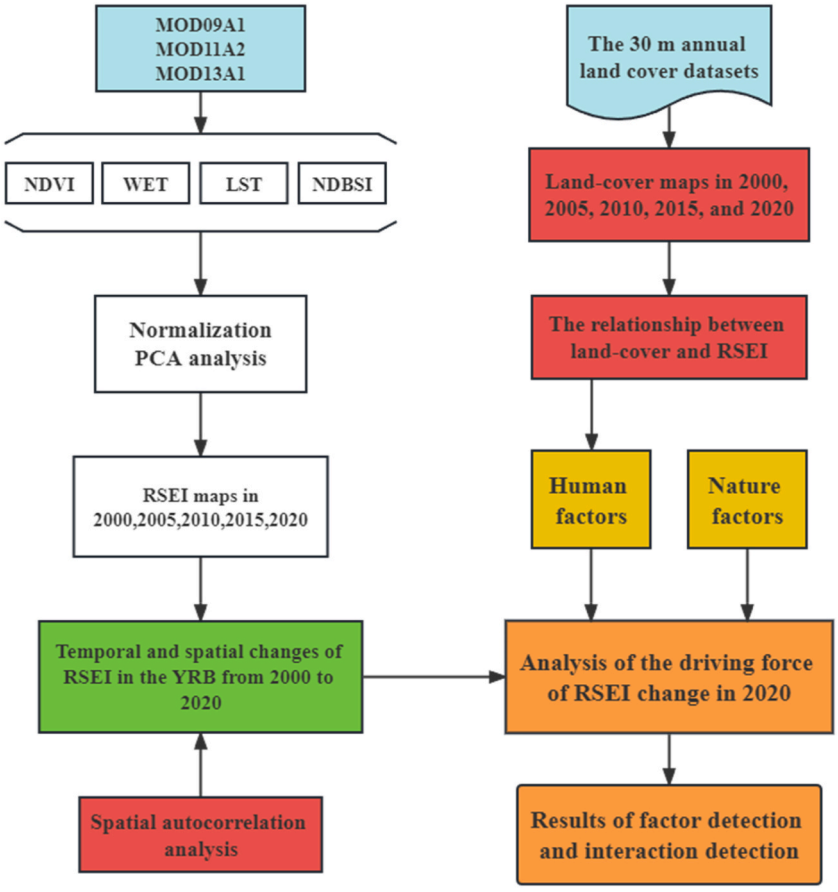

Fig. 2. The workflow diagram.

2.4. Research flow chart

The flowchart of the study is shown in Fig. 2.

3. Results

3.1. EEQ in the YRB

The RSEI number, which goes from 0 to 1, represents the EEQ, from poor to good. The yearly RSEI value is further split into 5 grades with 0.2 as the division value, which are poor (0–0.2), fair (0.2–0.4), moderate (0.4–0.6), good (0.6–0.8), and excellent (0.8–1.0), in order to more thoroughly analyze the regional variation of the EEQ in the YRB. The YRB's overall RSEI rating has been good for the past 20 years (Fig. 3(a–e)), and the EEQ in the center section of the basin is greater than in the upper and lower reaches, with the overall EEQ of the basin showing a constant improving trend. Most of the basin's RSEI was raised by one level between 2000 and 2010. In 2010, the EEQ in Sichuan, Shaanxi, and Hubei provinces all improved to "excellent" compared to 2000. In 2015, EEQ decreased slightly in the YRB, and the number of locations with "moderate" RSEI levels increased in the Jinsha River Basin and the YRD. Most places in Sichuan, Shaanxi, Yunnan, Guizhou, and Hubei achieved "excellent" EEQ levels in 2020, and the EEQ of the lower Yangtze River improved compared to 2010.

The proportion of places with RSEI ratings of "poor" and "fair" was the lowest in the research area for the 20-year period, both below 0.05 %. The share of the region with a "moderate" RSEI rating declined steadily from 11.57 % to 6.30 % between 2000 and 2010. Although the percentage of RSEI "good" areas declined by 15.41 % in 2010 compared to 2000, the percentage of "excellent" areas climbed by 20.7 %. The overall EEQ of the watershed fell somewhat in 2015, but the fraction of RSEI "moderate" area more than quadrupled to 12.50 %. In 2020, the proportion of "excellent" grade area was the highest in the last 20 years, at 45.12 %, while the percentage of "moderate" grade area was the lowest, at 5.79 %. Despite a modest decline in the average value of RSEI in the YRB in 2015, the general trend of RSEI in the YRB has been growing over the last 20 years, and the average value of RSEI in 2020 was the

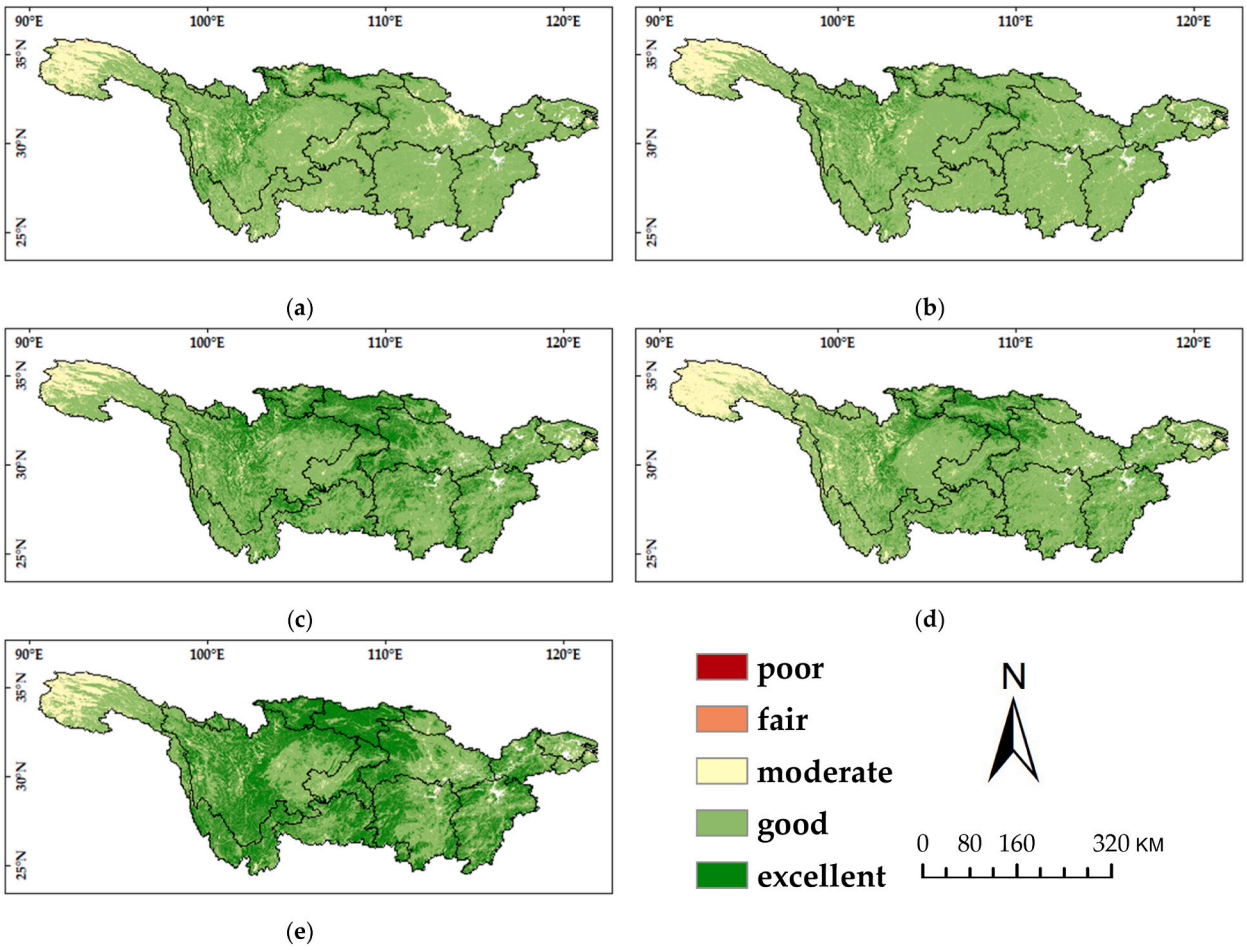

Fig. 3. Classification map of the EEQ in the YRB from 2000 to 2020. (**a**) 2000; (**b**) 2005; (**c**) 2010; (**d**) 2015; (**e**) 2020.

largest at 0.7719 (see Fig. 4).

3.2. Changes of EEQ in the YRB

To investigate the extent of changes in EEQ of the YRB from 2000 to 2020, EEQ was separated into two periods, 2000–2010 and 2010–2020, with 2010 serving as the dividing line. It is separated into "decrease by more than 2 levels", "decrease by 1 level", "no change", "increase by 1 level", and "increase by more than 2 levels", which correlate to "significantly worse", "worse", "unchanged", "better" and "significantly better". Table 1 displays the results.

Between 2000 and 2010, 4.53 % of the area had deteriorating EEQ, and 29.83 % had improved EEQ. From 2010 to 2020, 7.72 % of total areas had considerably deteriorating or worsening EEQ, whereas 23.58 % had significantly improved or better EEQ. When we compare the changes in EEQ area share between the two eras, we can observe that EEQ in the YRB increased from 2000 to 2010, but then slowed from 2010 to 2020. From 2000 to 2020, the total percentage of significantly worse and worse EEQ was 2.52 %, while the total percentage of significantly better and better EEQ was 43.20 %, indicating an increase in the YRB's overall EEQ.

Fig. 5(a–c) depicts the changes in EEQ level of the YRB. From 2000 to 2010, the EEQ in Shaanxi and Hubei provinces improved greatly, whereas the regions with declining EEQ were mostly concentrated in the middle section of Sichuan province. Between 2010 and 2020, regions with declining RSEI grades were mostly found in Henan and Hubei provinces, while EEQ increased by one grade in southern Sichuan and Yunnan provinces. Overall, the EEQ in most areas of the YRB has improved significantly, with most geographical RSEI grades upgraded from "good" to "excellent" in Gansu, Shaanxi, Guizhou, and Yunnan Province, but the natural environment in the YRD region is deteriorating.

3.3. Spatial variation characteristics of EEQ in YRB

3.3.1. Spatial characteristics based on the Global Moran's I index

Spatial autocorrelation analysis was done in ArcGIS. Due to the vast scope of the investigation and a limitation of computer memory, the remote sensing pictures were resampled using a fishing net technique to get 5500 sampling points and calculate the Global Moran's I index during the research period in the YRB. This enabled the investigation of the geographical aspects of EEQ variations in YRB. The z-statistic of the Global Moran's I index was determined to be positive, suggesting that the geographical distribution of EEQ changes in the research region was significantly aggregated rather than random. The five-period photos had indices of 0.52, 0.46, 0.54, 0.64, and 0.66, respectively.

3.3.2. Spatial characteristics based on the Local Moran's I index

Using high-low clustering analysis, the RSEI of the YRB was grouped and divided into five groups: insignificant, high-high clustering (H–H), low-low clustering (L-L), high-low clustering (H-L), and low-high clustering (L-H). For the past 20 years, in the YRB, the spatial aggregation features of EEQ are mostly high-high clustering and low-low clustering. According to Fig. 6(a–e), from 2000 to 2020, the overall high-high clusters with superior EEQ in the YRB are located in Shaanxi and Gansu provinces, while the low-low clusters with poor EEQ are dispersed in Qinghai province. It is worth noting that several types of agglomeration have emerged in western Sichuan over the past 20 years, indicating a more complicated distribution of EEQ in the region. The spatial distribution of EEQ in the YRB was relatively stable before 2015, and the expansion of high-high agglomeration area in Gansu, Shaanxi and western Sichuan after 2015 suggests that there is a trend of gradual improvement of EEQ in the region; the area of low-low agglomeration in the YRD has increased, and the EEQ has deteriorated.

3.4. The relationship between land use change and RSEI

The most fundamental and visible landscape characteristic representing the influence of human activities on the disruption of the Earth's surface is land use change [47]. When compared to other socioeconomic indicators, it is the most vulnerable to change. It is

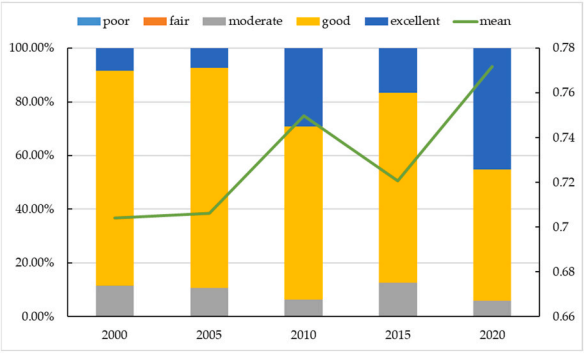

Fig. 4. EEQ's grade area and proportion of the YRB.

Table 1
Changes in ecologic conditions in the YRB from 2000 to 2020.

Year	2000–2010		2010–2020		2000–2020	
Change	Area (km^2)	Percent (%)	Area (km^2)	Percent (%)	Area (km^2)	Percent (%)
Significantly worse	2819.92	0.16 %	1691.46	0.10 %	648.87	0.04 %
Worse	77741.28	4.37 %	135439.90	7.62 %	44022.01	2.48 %
Unchanged	1167345.98	65.64 %	1221534.43	68.70 %	965367.46	54.29 %
Better	515304.72	28.98 %	408293.15	22.96 %	737110.71	41.45 %
Significantly better	15165.77	0.85 %	10987.14	0.62 %	31035.51	1.75 %

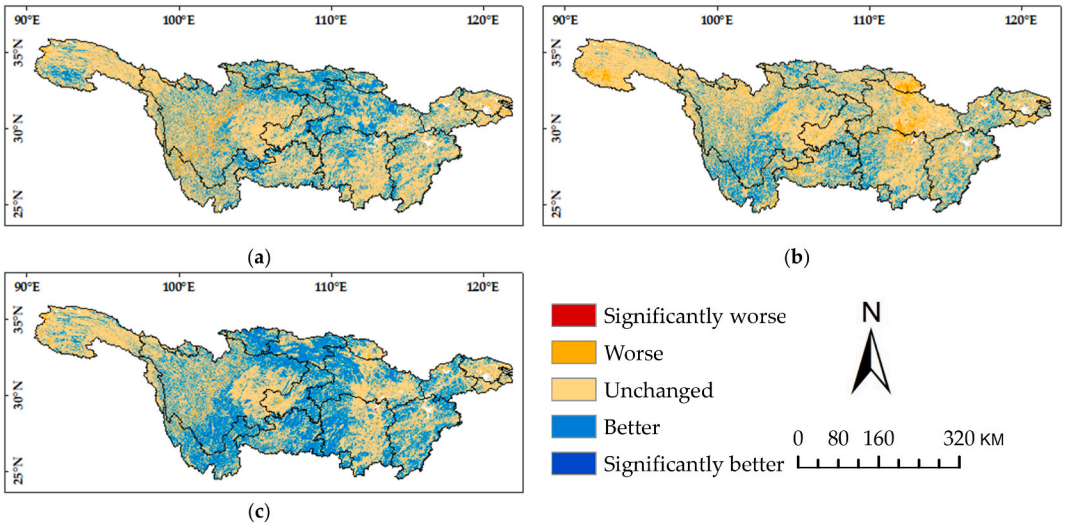

Fig. 5. Changes in ecologic conditions in the YRB from 2000 to 2020. (a) 2000–2010; (b) 2010-242 2020; (c) 2000–2020.

worth mentioning that the biological abundance index is generated from the land use type, and the effect of biological abundance on ecosystem quality is ranked third in the one-factor test with a q-value of 0.5. It suggests that land use has a significant impact on the watershed's natural environment. As a result, the link between land use and RSEI has been thoroughly investigated. Combining the YRB land use map for the past 20 years (Table 2), it is clear that the YRB's land use has changed dramatically between 2000 and 2020. Cropland, shrub, and grassland declined in extent, whereas forest, barren, and impervious surface grew. In 2020, the forest area had the maximum proportion of 46.52 %, compared to the lowest percentage of 45.41 % in 2000. The impervious surface consists mostly of urban and building areas in the YRD, Middle Yangtze River Plain, and Chengdu Plain. From 2000 to 2020, the impervious surface growth rate of 1.29 % was the highest among land use categories, negatively impacting RSEI. Among the land use classifications whose area dropped, cropland had the highest decrease rate, followed by grassland, with decrease rates of −1.50 % and −1.02 %, respectively. The diminished farming and grassland area was mostly converted into forest and agricultural land. Finally, the area of barren land and water did not change considerably, confirming prior findings [48,49].

Fig. 7 shows the average RSEI values for different land use categories. The average RSEI values of each land use type varied, and the RSEI of each land use type generally increased from 2000 to 2020. In 2020, the RSEI values of forest and shrub exceeded 0.8; the average RSEI values for the study years were 0.768 and 0.752, both greater than 0.75; and the average RSEI values were the highest of all land use categories. The RSEI values for cropland and wetland were above 0.7, with 0.724 and 0.744 respectively. Barren is the most environmentally vulnerable land use class [50], having the lowest average RSEI value of 0.53.

3.5. Factors influencing the EEQ of the YRB

3.5.1. Diversity and factor detection

To examine the influencing elements of EEQ in the research region, soil sand content, biological abundance index, annual precipitation, average annual temperature, elevation, population density, GDP, night lighting, and point-of-interest data were chosen as independent variables (influencing factors). Fig. 8 depicts the results of the factor detector. In 2020, the following are the degrees of effect of each detection factor on the regional distribution of the EEQ: Population density > GDP > biological abundance index > night lighting > point-of-interest > elevation >average annual temperature > soil sand content > annual precipitation. Population density, GDP, night lighting, and points of interest were four of the top five socioeconomic factors. This suggests that human activities had a stronger influence on the region's ecological quality. The biological abundance index and elevation had explanatory powers of 0.50 and 0.39, respectively, whereas the other natural determinants had explanatory powers of less than 0.2.

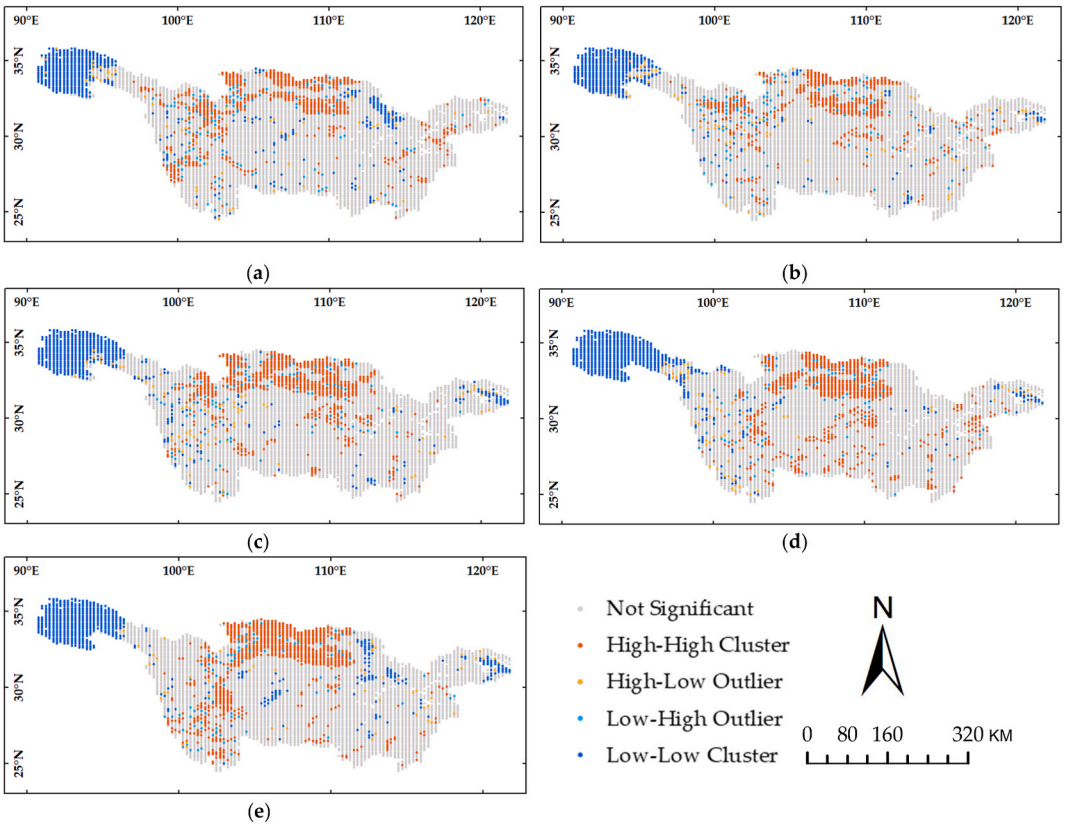

Fig. 6. LISA aggregation in the YRB from 2000 to 2020. (**a**) 2000; (**b**) 2005; (**c**) 2010; (**d**) 2015; (**e**) 2020.

Table 2
Statistical results of different land types in the YRB from 2000 to 2020.

Land use types	Proportion of the Corresponding Area					Range of variation
	2000	2005	2010	2015	2020	
Cropland	30.19 %	29.76 %	29.47 %	29.13 %	28.69 %	−1.50 %
Forest	45.41 %	45.76 %	45.89 %	45.94 %	46.52 %	1.11 %
Shrub	0.69 %	0.70 %	0.69 %	0.57 %	0.53 %	−0.17 %
Grassland	19.35 %	19.09 %	18.82 %	18.77 %	18.33 %	−1.02 %
Water	2.01 %	2.06 %	2.12 %	2.17 %	2.07 %	0.06 %
Snow/Ice	0.17 %	0.17 %	0.20 %	0.17 %	0.14 %	−0.03 %
Barren	0.99 %	1.03 %	1.02 %	1.08 %	1.25 %	0.25 %
Impervious	1.19 %	1.43 %	1.78 %	2.17 %	2.48 %	1.29 %
Wetland	0.00 %	0.00 %	0.00 %	0.00 %	0.00 %	0.00 %

3.5.2. Interaction detection

Interaction detection is carried out on the elements that have been chosen to examine the extent of influence on the EEQ when any two factors work together. To better understand how different components interact, interaction detection can also provide the direction, strength, and linearity of an interaction. Fig. 9 displays the outcomes of the factor interaction detection in this study. All of the results of the factor interaction detection demonstrate a two-factor increased or non-linear enhanced effect, indicating that the impact on the EEQ is better explained by the two-factor interaction than by the single factor.

With a q-value of 0.737 in 2020, the interaction between the biological abundance index and population density had the most effect, followed by the interaction between the biological abundance index and GDP with a q-value of 0.733. As seen in Fig. 9, the interaction of each driver with the biological abundance index resulted in a considerable rise in q values. Although annual precipitation and average annual temperatures had a minor impact on the ecological environment of the YRB in the univariate analysis, the q-value of the interaction between the two and the biological abundance index increased significantly under the interaction detection.

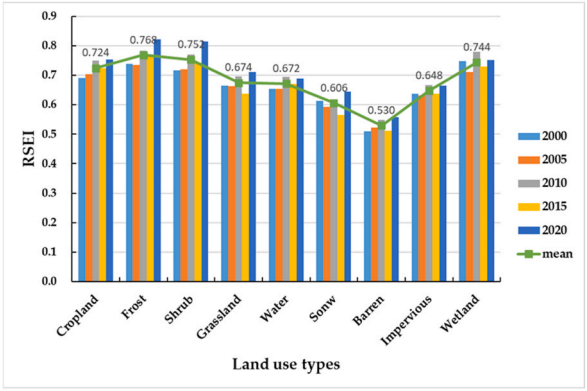

Fig. 7. Mean RSEI values of each land use types.

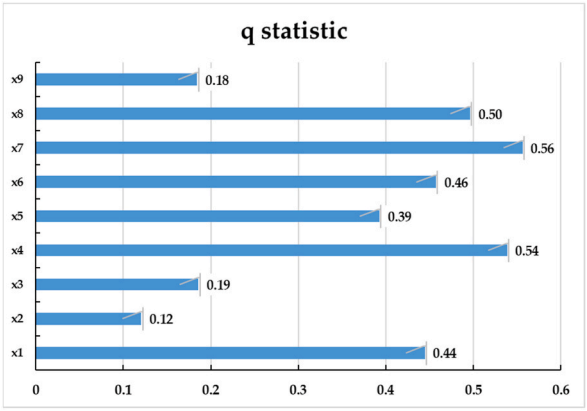

Fig. 8. Results of factor detector. ×1: point-of-interest; ×2: annual precipitation; ×3: average annual temperature; ×4: GDP; ×5: elevation; ×6: night lighting; ×7: population density; ×8: biological abundance index; ×9: soil sand content.

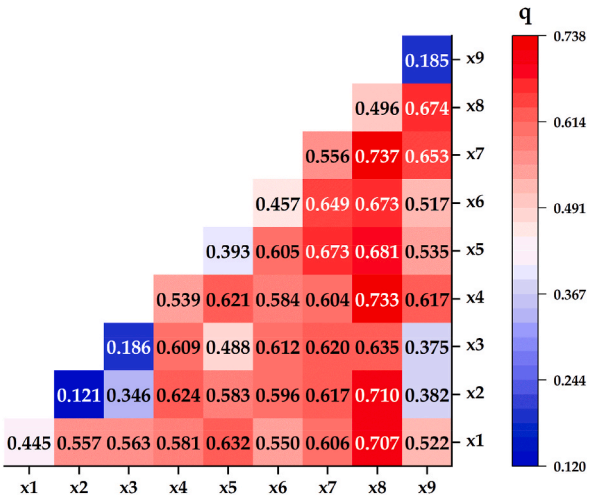

Fig. 9. Interaction detection results. ×1: point-of-interest; ×2: annual precipitation; ×3: average annual temperature; ×4: GDP; ×5: elevation; ×6: night lighting; ×7: population density; ×8: biological abundance index; ×9: soil sand content.

4. Discussion

4.1. Comparison with existing results

The YRB's EEQ is the consequence of a combination of natural and human made causes, and the study's findings demonstrate that the YRB's summer RSEI has shown a tendency of growing, then falling, and then increasing during the last 20 years. Overall, the EEQ of the YRB is improving, which is consistent with the findings of Yang et al. [36]. The EEQ of the lower Yangtze River is generally high and has increased steadily from 2000 to 2015, which is consistent with the findings of He [51] and Zheng [52]. The EEQ in the higher parts of the Yangtze River improved before deteriorating somewhat, which was consistent with Zhang's findings [1]. The government must address this issue and provide ecological restoration methods as quickly as possible. This is especially evident when considering the Chengdu-Chongqing urban agglomeration's poor biological environment downstream of the Jialing River [53]. The EEQ in the Yangtze River's middle reaches revealed an overall improving trend, which was consistent with Tian's findings [54].

This paper chooses driving factors such as climate factor, elevation, soil, nighttime light index, and POI data to quantitatively analyze the driving mechanisms of natural conditions and human activities on EEQ changes via GeoDetector based on the analysis of spatial and temporal changes in EEQ. The driving elements chosen in this work are more thorough, scientific, and suited for exploring the driving mechanisms of EEQ changes than Yang et al.'s livestock stocking quantity and topographic features [36]. Human activities are the primary cause of ecological changes in the watershed, according to an analysis of the influence of various drivers on ecological flows. The socio-economic factors that have the greatest impact on the ecology of the watershed are GDP, population density, and the biological abundance index, while elevation is the natural factor that has the greatest impact on the EEQ [54,55].

4.2. Discussion of spatial correlation features

Various types of agglomeration have emerged in western Sichuan in the past 20 years, showing that the distribution of EEQ in the region is complicated, which may be related to the region's vast topographic relief and complex ecological conditions. Before 2015, the geographical distribution of EEQ in the YRB was generally stable, and the development of the high-altitude agglomeration area in Gansu, Shaanxi and western Sichuan after 2015 means that the region's EEQ is gradually improving. The implementation of key national ecological protection initiatives, such as the "Three-North" protective forest system project, the natural forest protection project and the farmland-to-forest-to-grassland project, has begun to bear fruit. Since 2010, the YRD region has been confronted with the degradation of the EEQ, which is related to the rapid growth of the YRD. Human activities have a greater impact on the region's biological environment than natural forces. Although the original EEQ of the YRD region was quite acceptable, a number of environmental problems such as water and air pollution caused by urbanization and development have led to a decline in the EEQ of the YRD region.

4.3. Relationship between land-use types and EEQ

Several studies have shown that vegetation can successfully prevent soil erosion, thereby increasing the resilience and carrying capacity of the ecological environment [51]. From 2000 to 2020, the area of forest increased by 1.11%, mainly in Gansu and Shaanxi provinces, where the ecological situation has improved significantly. Human activities and social growth have exacerbated land cover changes, and pollution from industrial expansion has damaged the surrounding ecology. In order to meet the demand for land for economic growth, a considerable amount of arable land in the YRD region has been occupied and the area of impervious surface has increased dramatically, which is consistent with the deteriorating trend in the EEQ of the YRD region. Therefore, for the long-term growth of the regional ecological environment, it is necessary to strengthen the conservation of forests, grasslands and other vegetation in the study area, as well as scientific and reasonable land use planning.

4.4. Response of RSEI to natural factors

Elevation, annual precipitation, and average annual temperature were the three categories of natural elements that were chosen for the study. According to the findings of the geographic probing study, elevation is the natural component that has the greatest impact on the YRB's EEQ. The YRB's topography follows a pattern of high in the west and low in the east across the three main terrains of Chinese topography. According to Yang's findings [36], high-altitude regions with large topographic relief and slope, complex terrain, relatively homogeneous vegetation types, and extremely fragile ecological environments that are vulnerable to degradation include the Hengduan Mountains in the Jinsha River Basin and the Minto River Basin. The Yangtze River's source and upstream regions, where natural forces are the primary driving force, should pay sufficient attention to ecological engineering buildings [56]. The EEQ in the southern Jialing River Basin, Dongting Lake Basin, Poyang Lake Basin, and YRD is "good" and "excellent" since these regions are low in elevation, primarily plain and hilly, and have a climate that supports the growth of plants [37].

4.5. Response of RSEI to socioeconomic factors

Although the region's EEQ has remained stable as a result of many policies, including the establishment of the Sanjiangyuan Nature Reserve and the implementation of the grassland ecological protection compensation policy, human activities in the Jinsha River Basin's Heng-duan Mountains, such as grazing and excessive lawn development, have contributed to the degradation of the EEQ to

some extent [57]. In the middle and lower portions of the YRB, rising urbanization has caused an annual increase in population density since 1990, affecting local land use and vegetation change [58,59]. The ecological environment is under stress as a result of urbanization, population growth, industrial concentration, resource and energy use, and geographic expansion [60–63]. According to the findings [64], urban growth reduced the amount of productive land in the YRB, which resulted in an increase in construction land, a decrease in plant diversity, and a reduction in vegetation cover, particularly in the Chengdu-Chongqing urban agglomeration and the YRD, which is in line with Qu's findings [65].

4.6. Limitations and uncertainties

This study provides a strong scientific framework for quick evaluation of EEQ in the YRB and other watersheds, although the RSEI calculation and driving mechanism analysis in this paper are still lacking. The principal component analysis computation of RSEI is unstable and cannot guarantee a large contribution [66]. In subsequent research, the computation of RSEI may be improved by employing the entropy value approach to address the issue of insufficient data consumption. For the past 20 years, the article has examined the regional and temporal changes in EEQ in the YRB. Due to the large amount of data and time-consuming processing, the five data periods from 2000, 2005, 2010, 2015, and 2020 were chosen for the study based on systematic and holistic as well as scientific considerations, and the results lacked precision when compared to the data analysis results of 20 consecutive years, so relevant studies can be conducted later using continuous time series.

5. Conclusions

The RSEI was employed in this study to measure the YRB's total EEQ based on the GEE platform. The findings of the analysis revealed:

5. The YRB's mean RSEI varied from 0.70 to 0.77 for the five monitoring years from 2000 to 2020. The overall EEQ was mostly good; there is significant spatial heterogeneity of RSEI in the YRB, and the EEQ in most areas of Qinghai Province has always been medium, while it has always been good in the YRD. The EEQ of Shaanxi, Gansu, Yunnan, and western Sichuan provinces has improved dramatically since 2000.
6. According to the spatial correlation analysis, the type of EEQ aggregation in Gansu and Shaanxi provinces has been high-high aggregation, and the area of aggregation has been expanding, indicating that the region's EEQ has been improving. The low-aggregation regions are concentrated in Qinghai Province and the YRD, the former because of natural factors restricting the delicate biological environment and the latter because of urbanization.
7. Population density, GDP and the bio abundance index all had q-values greater than 0.5, indicating that these three factors had the greatest effect on regional EEQ. With the q-value of 0.737, the bio abundance index interacted with population density to have the largest effect on regional EEQ. This study investigated the impact of different factors on the EEQ of the YRB, which means that more attention should be paid to the environmental impact of human activities in the ecological management process of the YRB.

Funding

This research was funded by the National Natural Science Foundation of China (Grant No. 41701477) and the Jiangsu Province Social Science Foundation, China (Grant No. 22GLD007).

Data availability statement

Data will be made available on request.

CRediT authorship contribution statement

Zixi Liu: Writing – original draft, Validation, Methodology, Formal analysis, Conceptualization. **Weiwei Zhang:** Writing – review & editing, Supervision, Resources, Investigation, Conceptualization. **Huiyuan Lu:** Writing – review & editing, Validation. **Jianwan Ji:** Writing – review & editing. **Zhaohui Yang:** Writing – review & editing. **Chao Chen:** Writing – review & editing.

Declaration of competing interest

The authors declare that they have no known competing financial interests or personal relationships that could have appeared to influence the work reported in this paper.

Acknowledgements

We would like to thank the editor and anonymous reviewers for their constructive comments and suggestions for improving the manuscript.

References

[1] J. Zhang, L. Yang, E. Gong, Y. Wang, J. Ren, M. Liu, Dynamic monitoring of eco-environmental quality in Xi'an based on GEE and adjusted RSEI, Acta Ecol. Sin. 43 (2023) 2114–2127. https://kns.cnki.net/kcms/detail/11.2031.Q.20221020.1135.040.html.

[2] C. Zhang, S. Yang, X. Dong, C. Zhao, H. Bo, J. Liu, Research on spatiotemporal evolution and influencing factors of ecological environment quality in the upper Yangtze River Basin based on RSEI index, Res. Soil Water Conserv. 30 (2023) 356–363, https://doi.org/10.13869/j.cnki.rswc.20220601.005.

[3] C.N. Cook, M. Hockings, Opportunities for improving the rigor of management effectiveness evaluations in protected areas, Conserv Lett 4 (2011) 372–382, https://doi.org/10.1111/j.1755-263X.2011.00189.x.

[4] D.B. Lindenmayer, G.E. Likens, The science and application of ecological monitoring, Biol. Conserv. 143 (2010) 1317–1328, https://doi.org/10.1016/j.biocon.2010.02.013.

[5] N. Pettorelli, W.F. Laurance, T.G. O'Brien, M. Wegmann, H. Nagendra, W. Turner, Satellite remote sensing for applied ecologists: opportunities and challenges, J. Appl. Ecol. 51 (2014) 839–848, https://doi.org/10.1111/1365-2664.12261.

[6] X.-P. Zhang, X.-M. Cheng, Energy consumption, carbon emissions, and economic growth in China, Ecol. Econ. 68 (2009) 2706–2712, https://doi.org/10.1016/j.ecolecon.2009.05.011.

[7] G. Shi, T. Dai, N. Xu, Latest progress of the study of atmospheric CO_2 concentration retrievals from satellite, Adv. Earth Sci. (2010) 7–13.

[8] R.K. Pachauri, M.R. Allen, V.R. Barros, J. Broome, W. Cramer, R. Christ, J.A. Church, L. Clarke, Q. Dahe, P. Dasgupta, N.K. Dubash, O. Edenhofer, I. Elgizouli, C. B. Field, P. Forster, P. Friedlingstein, J. Fuglestvedt, L. Gomez-Echeverri, S. Hallegatte, G. Hegerl, M. Howden, K. Jiang, B. Jimenez Cisneroz, V. Kattsov, H. Lee, K.J. Mach, J. Marotzke, M.D. Mastrandrea, L. Meyer, J. Minx, Y. Mulugetta, K. O'Brien, M. Oppenheimer, J.J. Pereira, R. Pichs-Madruga, G.-K. Plattner, H.-O. Pörtner, S.B. Power, B. Preston, N.H. Ravindranath, A. Reisinger, K. Riahi, M. Rusticucci, R. Scholes, K. Seyboth, Y. Sokona, R. Stavins, T.F. Stocker, P. Tschakert, D. van Vuuren, J.-P. van Ypserle, Climate Change 2014: Synthesis Report. Contribution of Working Groups I, II and III to the Fifth Assessment Report of the Intergovernmental Panel on Climate Change, IPCC, Geneva, Switzerland, 2014. https://epic.awi.de/id/eprint/37530/.

[9] W.T. Tian, W.Y. Hu, J. Li, Z.L. Gao, The status of soil and water loss and analysis of countermeasures in China, Res. Soil Water Conserv. 15 (2008) 204–209.

[10] T. Newbold, L.N. Hudson, S.L.L. Hill, S. Contu, I. Lysenko, R.A. Senior, L. Börger, D.J. Bennett, A. Choimes, B. Collen, J. Day, A. De Palma, S. Díaz, S. Echeverria-Londoño, M.J. Edgar, A. Feldman, M. Garon, M.L.K. Harrison, T. Alhusseini, D.J. Ingram, Y. Itescu, J. Kattge, V. Kemp, L. Kirkpatrick, M. Kleyer, D.L.P. Correia, C.D. Martin, S. Meiri, M. Novosolov, Y. Pan, H.R.P. Phillips, D.W. Purves, A. Robinson, J. Simpson, S.L. Tuck, E. Weiher, H.J. White, R.M. Ewers, G.M. Mace, J.P. W. Scharlemann, A. Purvis, Global effects of land use on local terrestrial biodiversity, Nature 520 (2015) 45–50, https://doi.org/10.1038/nature14324.

[11] D.-Y. Miao, X.-D. Zhou, W. Cheng, Y. Li, The present situation analysis of environmental pollution and its control management in China, Water Conservancy Science and Technology and Economy 12 (2006) 751.

[12] P. Gonzalez, R.P. Neilson, J.M. Lenihan, R.J. Drapek, Global patterns in the vulnerability of ecosystems to vegetation shifts due to climate change, Global Ecol. Biogeogr. 19 (2010) 755–768, https://doi.org/10.1111/j.1466-8238.2010.00558.x.

[13] J. Kim, S. Kang, B. Seo, A. Narantsetseg, Y. Han, Estimating fractional green vegetation cover of Mongolian grasslands using digital camera images and MODIS satellite vegetation indices, GIsci Remote Sens 57 (2020) 49–59, https://doi.org/10.1080/15481603.2019.1662166.

[14] Q. Liu, Z. Yang, F. Han, Z. Wang, C. Wang, NDVI-based vegetation dynamics and their response to recent climate change: a case study in the Tianshan Mountains, China, Environ. Earth Sci. 75 (2016) 1189, https://doi.org/10.1007/s12665-016-5987-5.

[15] F. Yuan, M.E. Bauer, Comparison of impervious surface area and normalized difference vegetation index as indicators of surface urban heat island effects in Landsat imagery, Remote Sens. Environ. 106 (2007) 375–386, https://doi.org/10.1016/j.rse.2006.09.003.

[16] X. Luo, W. Li, Scale effect analysis of the relationships between urban heat island and impact factors: case study in Chongqing, J. Appl. Remote Sens. 8 (2014), 84995, https://doi.org/10.1117/1.JRS.8.084995.

[17] J. Hansen, R. Ruedy, M. Sato, K. Lo, Global surface temperature change, Rev. Geophys. 48 (2010), https://doi.org/10.1029/2010RG000345.

[18] S. Das, B. Pradhan, P.K. Shit, A.M. Alamri, Assessment of wetland ecosystem health using the pressure–state–response (PSR) model: a case study of mursidabad district of West Bengal (India), Sustainability 12 (2020) 5932. https://www.mdpi.com/2071-1050/12/15/5932.

[19] M. Sahana, M. Saini, G. Areendran, K. Imdad, K. Sarma, H. Sajjad, Assessing Wetland ecosystem health in Sundarban Biosphere Reserve using pressure-state-response model and geospatial techniques, Remote Sens. Appl. 26 (2022), 100754, https://doi.org/10.1016/j.rsase.2022.100754.

[20] M. Shi, H. Wu, X. Fan, H. Jia, T. Dong, P. He, M.F. Baqa, P. Jiang, Trade-offs and synergies of multiple ecosystem services for different land use scenarios in the yili river valley, China, Sustainability 13 (2021) 1577. https://www.mdpi.com/2071-1050/13/3/1577.

[21] Z. Wang, L. Xiao, H. Yan, Y. Qi, Q. Jiang, Optimization of the ecological network structure based on scenario simulation and trade-offs/synergies among ecosystem services in nanping, Rem. Sens. 14 (2022) 5245. https://www.mdpi.com/2072-4292/14/20/5245.

[22] H. Huang, W. Chen, Y. Zhang, L. Qiao, Y. Du, Analysis of ecological quality in lhasa metropolitan area during 1990–2017 based on remote sensing and Google Earth engine platform, J. Geogr. Sci. 31 (2021) 265–280, https://doi.org/10.1007/s11442-021-1846-8.

[23] S. Qureshi, S.K. Alavipanah, M. Konyushkova, N. Mijani, S. Fathololomi, M.K. Firozjaei, M. Homaee, S. Hamzeh, A.A. Kakroodi, A remotely sensed assessment of surface ecological change over the gomishan wetland, Iran, Rem. Sens. 12 (2020) 2989. https://www.mdpi.com/2072-4292/12/18/2989.

[24] Y. Jing, F. Zhang, Y. He, H. Kung, V.C. Johnson, M. Arikena, Assessment of spatial and temporal variation of ecological environment quality in ebinur lake wetland national nature reserve, xinjiang, China, Ecol. Indicat. 110 (2020), 105874, https://doi.org/10.1016/j.ecolind.2019.105874.

[25] X. Hu, H. Xu, A new remote sensing index for assessing the spatial heterogeneity in urban ecological quality: a case from Fuzhou City, China, Ecol. Indicat. 89 (2018) 11–21, https://doi.org/10.1016/j.ecolind.2018.02.006.

[26] J. Ji, Z. Tang, W. Zhang, W. Liu, B. Jin, X. Xi, F. Wang, R. Zhang, B. Guo, Z. Xu, E. Shifaw, Y. Xiong, J. Wang, S. Xu, Z. Wang, Spatiotemporal and multiscale analysis of the coupling coordination degree between economic development equality and eco-environmental quality in China from 2001 to 2020, Rem. Sens. 14 (2022) 737. https://www.mdpi.com/2072-4292/14/3/737.

[27] H. Xu, W. Duan, W. Deng, M. Lin, RSEI or MRSEI? Comment on Jia et al. Evaluation of Eco-Environmental Quality in Qaidam Basin Based on the Ecological Index (MRSEI) and GEE, Remote Sens. 2021, 13, 4543, Remote Sens (Basel) 14 (2022) 5307. https://www.mdpi.com/2072-4292/14/21/5307.

[28] J. Ji, Z. Tang, L. Jiang, T. Sheng, F. Zhao, R. Zhang, E. Shifaw, W. Liu, H. Li, X. Liu, H. Lu, Study on regional eco-environmental quality evaluation considering land surface and season differences: a case study of zhaotong city, Rem. Sens. 15 (2023) 657. https://www.mdpi.com/2072-4292/15/3/657.

[29] X. Niu, Y. Li, Remote Sensing Evaluation of Ecological Environment of Anqing City Based on Remote Sensing Ecological Index, the International Archives of the Photogrammetry, Remote Sensing and Spatial Information Sciences. XLIII-B3-2020, 2020, pp. 733–737, https://doi.org/10.5194/isprs-archives-XLIII-B3-2020-733-2020.

[30] O. Mutanga, L. Kumar, Google Earth engine applications, Rem. Sens. 11 (2019) 591. https://www.mdpi.com/2072-4292/11/5/591.

[31] J. Xiong, P.S. Thenkabail, M.K. Gumma, P. Teluguntla, J. Poehnelt, R.G. Congalton, K. Yadav, D. Thau, Automated cropland mapping of continental Africa using Google Earth Engine cloud computing, ISPRS J. Photogrammetry Remote Sens. 126 (2017) 225–244, https://doi.org/10.1016/j.isprsjprs.2017.01.019.

[32] M. Campos-Taberner, Á. Moreno-Martínez, F.J. García-Haro, G. Camps-Valls, N.P. Robinson, J. Kattge, S.W. Running, Global estimation of biophysical variables from Google Earth engine platform, Rem. Sens. 10 (2018) 1167. https://www.mdpi.com/2072-4292/10/8/1167.

[33] X. Hou, T. Wu, L. Yu, S. Qian, Characteristics of multi-temporal scale variation of vegetation coverage in the Circum Bohai Bay Region, 1999–2009, Acta Ecol. Sin. 32 (2012) 297–304, https://doi.org/10.1016/j.chnaes.2012.08.001.

[34] S. Qu, L. Wang, A. Lin, H. Zhu, M. Yuan, What drives the vegetation restoration in Yangtze River basin, China: climate change or anthropogenic factors? Ecol. Indicat. 90 (2018) 438–450, https://doi.org/10.1016/j.ecolind.2018.03.029.

[35] J. Zhang, A. Zhang, M. Song, Ecological benefit spillover and ecological financial transfer of cultivated land protection in river basins: a case study of the Yangtze River economic belt, China, Sustainability 12 (2020) 7085. https://www.mdpi.com/2071-1050/12/17/7085.

[36] X. Yang, F. Meng, P. Fu, Y. Zhang, Y. Liu, Spatiotemporal change and driving factors of the eco-environment quality in the Yangtze River Basin from 2001 to 2019, Ecol. Indicat. 131 (2021), https://doi.org/10.1016/j.ecolind.2021.108214.

[37] X.C. Ye, X.X. Yang, F.H. Liu, J. Wu, J. Liu, Spatio-temporal variations of land vegetation gross primary production in theYangtze River Basin and correlation with meteorological factors, Acta Ecol. Sin. (2021) 1–11.
[38] S. Zhang, P. Yang, J. Xia, K. Qi, W. Wang, W. Cai, N. Chen, Research and analysis of ecological environment quality in the, Middle Reaches of the Yangtze River Basin between 2000 and 2019 13 (2021) 4475. https://www.mdpi.com/2072-4292/13/21/4475.
[39] Y. Wu, K. Shi, Z. Chen, S. Liu, Z. Chang, Developing improved time-series DMSP-OLS-like data (1992–2019), China by Integrating DMSP-OLS and SNPP-VIIRS, IEEE Transactions on Geoscience and Remote Sensing 60 (2022) 1–14, https://doi.org/10.1109/TGRS.2021.3135333.
[40] H. Xu, A remote sensing index for assessment of regional ecological changes, China Environ. Sci. 33 (2013) 889–897.
[41] S. Huang, L. Tang, J.P. Hupy, Y. Wang, G. Shao, A commentary review on the use of normalized difference vegetation index (NDVI) in the era of popular remote sensing, J. Res. 32 (2021) 1–6, https://doi.org/10.1007/s11676-020-01155-1.
[42] Y. Zhao, Z. Qu, Y. Zhang, Y. Ao, L. Han, S. Kang, Y. Sun, Effects of Human Activity Intensity on Habitat Quality Based on Nighttime Light Remote Sensing: A Case Study of Northern Shaanxi, China, Science of the Total Environment. 851, 2022, 158037, https://doi.org/10.1016/j.scitotenv.2022.158037.
[43] J. Wang, C. Xu, Geodetector: principle and prospective, Acta Geograph. Sin. 72 (2017) 116–134.
[44] L. Zhu, J. Meng, L. Zhu, Applying Geodetector to disentangle the contributions of natural and anthropogenic factors to NDVI variations in the middle reaches of the Heihe River Basin, Ecol. Indicat. 117 (2020), 106545, https://doi.org/10.1016/j.ecolind.2020.106545.
[45] H. Huo, C. Sun, Spatiotemporal variation and influencing factors of vegetation dynamics based on Geodetector: a case study of the northwestern Yunnan Plateau, China, Ecol. Indicat. 130 (2021), 108005, https://doi.org/10.1016/j.ecolind.2021.108005.
[46] Y. Wang, Z. Zhang, X. Chen, Quantifying influences of natural and anthropogenic factors on vegetation changes based on geodetector: a case study in the Poyang Lake Basin, China, Rem. Sens. 13 (2021) 5081. https://www.mdpi.com/2072-4292/13/24/5081.
[47] C. Liu, W. Li, G. Zhu, H. Zhou, H. Yan, P. Xue, Land use/land cover changes and their driving factors in the northeastern Tibetan plateau based on geographical detectors and Google Earth engine, A Case Study in Gannan Prefecture 12 (2020) 3139. https://www.mdpi.com/2072-4292/12/19/3139.
[48] L. He, W. Li, S. Tian, H. Zheng, Analysis of the impact of rapid urbanization on farmland protection in the Yangtze River Economic Belt, Acta Ecol. Sin. 38 (2018) 7782–7789. https://kns.cnki.net/kcms/detail/11.2031.Q.20180808.1352.004.html.
[49] L. Kong, L. Zhang, H. Zheng, W. Xu, Y. Xiao, Z. Ouyang, Driving forces behind ecosystem spatial changes in the Yangtze River Basin, Acta Ecol. Sin. 38 (2018) 741–749.
[50] J. Zhang, G. Yang, L. Yang, Z. Li, M. Gao, C. Yu, E. Gong, H. Long, H. Hu, Dynamic monitoring of environmental quality in the loess plateau from 2000 to 2020 using the Google Earth engine platform and the remote sensing, Ecological Index 14 (2022) 5094. https://www.mdpi.com/2072-4292/14/20/5094.
[51] T. He, N. Tian, R. Zhou, Q. Ma, J. Zhang, J. Gao, Dynamic assessment of eco-environmental quality in Yangtze River Delta integration demonstration area based on GEE and RSEI, Chinese Journal of Ecology 42 (2023) 436–444, https://doi.org/10.13292/j.1000-4890.202302.017.
[52] Z. Zheng, Z. Wu, Y. Chen, Z. Yang, F. Marinello, Analyzing the ecological environment and urbanization characteristics of the Yangtze River Delta urban agglomeration based on Google Earth engine, Acta Ecol. Sin. 41 (2021) 717–729. https://kns.cnki.net/kcms/detail/11.2031.Q.20201127.0938.046.html.
[53] X. Wu, X. Fan, X. Liu, L. Xiao, Q. Ma, N. He, Si Gao, Y. Qiao, Temporal and spatial changes of ecological quality of Chengdu-Chongqing Urban Agglomeration based on Google Earth Engine cloud platform, Chinese Journal of Ecology 42 (2023) 759–768, https://doi.org/10.13292/j.1000-4890.202303.009.
[54] Z. Tian, C. Yin, X. Wang, Dynamic monitoring and driving factors analysis of ecological environment quality in Poyang Lake Basin, Environ. Sci. J. Integr. Environ. Res. 44 (2023) 816–827, https://doi.org/10.13227/j.hjkx.202201097.
[55] W. Li, X. Ren, Z. Zhou, Research on the Ecological Environment Quality Change and Influencing Factors of Chishui River Basin in Guizhou Based on Remote Sensing Ecological Index, 2022, https://doi.org/10.27048/d.cnki.ggzsu.2022.000093.
[56] H. Liu, It is difficult for China's greening through large-scale afforestation to cross the Hu Line, Sci. China Earth Sci. 62 (2019) 1662–1664, https://doi.org/10.1007/s11430-019-9381-3.
[57] Y. Deng, S. Yao, M. Hou, T. Zhang, Temporal and spatial variation of vegetation NDVI and its topographic differentiation effect in the middle and upper reaches of the Yangtze River Basin, Resour. Environ. Yangtze Basin 29 (2020) 66–78.
[58] L. Olsson, L. Eklundh, J. Ardö, A recent greening of the Sahel—trends, patterns and potential causes, J. Arid Environ. 63 (2005) 556–566, https://doi.org/10.1016/j.jaridenv.2005.03.008.
[59] K. Van der Geest, A. Vrieling, T. Dietz, Migration and environment in Ghana: a cross-district analysis of human mobility and vegetation dynamics, Environ. Urbanization 22 (2010) 107–123, https://doi.org/10.1177/0956247809362842.
[60] L. Aldieri, C.P. Vinci, Green economy and sustainable development: the economic impact of innovation on employment, Sustainability 10 (2018) 3541. https://www.mdpi.com/2071-1050/10/10/3541.
[61] L. Fei, Z. Shuwen, Y. Jiuchun, B. Kun, W. Qing, T. Junmei, C. Liping, The effects of population density changes on ecosystem services value: a case study in Western Jilin, China, Ecol. Indicat. 61 (2016) 328–337, https://doi.org/10.1016/j.ecolind.2015.09.033.
[62] X. Jia, B. Fu, X. Feng, G. Hou, Y. Liu, X. Wang, The tradeoff and synergy between ecosystem services in the Grain-for-Green areas in Northern Shaanxi, China, Ecol. Indicat. 43 (2014) 103–113, https://doi.org/10.1016/j.ecolind.2014.02.028.
[63] C. Yang, Q. Lu, L. Xie, Rural-urban migration, rural household income and local geographical contexts - a case of northwestern Guangxi, China, Chin. Geogr. Sci. 18 (2008) 17–23, https://doi.org/10.1007/s11769-008-0017-5.
[64] A.F. Barbieri, D.L. Carr, Gender-specific out-migration, deforestation and urbanization in the Ecuadorian Amazon, Global Planet. Change 47 (2005) 99–110, https://doi.org/10.1016/j.gloplacha.2004.10.005.
[65] S. Qu, L. Wang, A. Lin, D. Yu, M. Yuan, C. Li, Distinguishing the impacts of climate change and anthropogenic factors on vegetation dynamics in the Yangtze River Basin, China, Ecol. Indicat. 108 (2020), 105724, https://doi.org/10.1016/j.ecolind.2019.105724.
[66] Y. Li, Z. Li, J. Wang, H. Zeng, Analyses of driving factors on the spatial variations in regional eco-environmental quality using two types of species distribution models: a case study of Minjiang River Basin, China, Ecol. Indicat. 139 (2022), 108980, https://doi.org/10.1016/j.ecolind.2022.108980.